

Influence of Affinity and Antigen Internalization on the Uptake and Penetration of Anti-HER2 Antibodies in Solid Tumors

Stephen I. Rudnick¹, Jianlong Lou³, Calvin C. Shaller¹, Yong Tang⁴, Andres J.P. Klein-Szanto², Louis M. Weiner⁴, James D. Marks³, and Gregory P. Adams¹

Abstract

Antibody drugs are widely used in cancer therapy, but conditions to maximize tumor penetration and efficacy have yet to be fully elucidated. In this study, we investigated the impact of antibody binding affinity on tumor targeting and penetration with affinity variants that recognize the same epitope. Specifically, we compared four derivatives of the C6.5 monoclonal antibody (mAb), which recognizes the same HER2 epitope (monovalent K_D values ranging from 270 to 0.56 nmol/L). Moderate affinity was associated with the highest tumor accumulation at 24 and 120 hours after intravenous injection, whereas high affinity was found to produce the lowest tumor accumulation. Highest affinity mAbs were confined to the perivascular space of tumors with an average penetration of $20.4 \pm 7.5 \mu\text{m}$ from tumor blood vessels. Conversely, lowest affinity mAbs exhibited a broader distribution pattern with an average penetration of $84.8 \pm 12.8 \mu\text{m}$. *In vitro* internalization assays revealed that antibody internalization and catabolism generally increased with affinity, plateauing once the rate of HER2 internalization exceeded the rate of antibody dissociation. Effects of internalization and catabolism on tumor targeting were further examined using antibodies of moderate (C6.5) or high-affinity (trastuzumab), labeled with residualizing (¹¹¹In-labeled) or nonresidualizing (¹²⁵I-labeled) radioisotopes. Significant amounts of antibody of both affinities were degraded by tumors *in vivo*. Furthermore, moderate- to high-affinity mAbs targeting the same HER2 epitope with monovalent affinity above 23 nmol/L had equal tumor accumulation of residualizing radiolabel over 120 hours. Results indicated equal tumor exposure, suggesting that mAb penetration and retention in tumors reflected affinity-based differences in tumor catabolism. Together, these results suggest that high-density, rapidly internalizing antigens subject high-affinity antibodies to greater internalization and degradation, thereby limiting their penetration of tumors. In contrast, lower-affinity antibodies penetrate tumors more effectively when rates of antibody-antigen dissociation are higher than those of antigen internalization. Together, our findings offer insights into how to optimize the ability of therapeutic antibodies to penetrate tumors. *Cancer Res*; 71(6); 2250–9. ©2011 AACR.

Introduction

Tumor-targeting specificity of monoclonal antibodies (mAb) requires the target antigen to be solely or primarily expressed on the tumor cells, whereas efficacy requires sufficient binding affinity of the mAb to mediate durable tumor

retention. These principles have led to the commonly held concept that mAb must have high affinity in order to be therapeutically relevant.

Weinstein's modeling of the micropharmacology of antibodies in solid tumors began to redirect the focus in antibody development away from generating antibodies with very high affinity. The "binding site barrier" model predicted that diffusion of high-affinity antibodies into tumors is limited because slow rates of dissociation decrease the local concentration of diffusible, free antibody (1, 2). The model predicts that as the strength of the bond between the mAb and its target increases, the amount of mAbs available to diffuse into tumor decreases, leading to a reduction in penetration into the tumor. This effect was hypothesized to be even more pronounced in tumor microenvironment where the lack of draining lymphatics hinders the diffusion of macromolecules (3). More recently, other models have predicted that antigen expression and internalization can have profound effects on mAb penetration in tumors due to internalization and catabolism (4, 5). Such

Authors' Affiliations: ¹Developmental Therapeutics Program and ²Pathology Department, Fox Chase Cancer Center, Philadelphia, Pennsylvania; ³Department of Anesthesia, University of California, San Francisco, California; and ⁴Lombardi Comprehensive Cancer Center, Georgetown University, Washington, District of Columbia

Note: Supplementary data for this article are available at Cancer Research Online (<http://cancerres.aacrjournals.org/>).

Corresponding Author: Gregory P. Adams, Fox Chase Cancer Center, 333 Cottman Avenue, W364, Philadelphia, PA 19111. Phone: 215-728-3890; Fax: 215-728-2741; E-mail: Gregory.Adams@fccc.edu

doi: 10.1158/0008-5472.CAN-10-2277

©2011 American Association for Cancer Research.

predictions have been verified *in vitro* by using tumor spheroid models (4).

Therapeutic antibodies exhibit limited tumor penetration and are often limited to perivascular spaces (6). Many studies have tested the predictions regarding affinity in models such as those described earlier (for review, see ref. 7). We previously conducted a comprehensive study that examined the role of affinity on *in vivo* tumor targeting by using a panel of anti-HER2 affinity mutant single-chain variable fragments (scFv; ref. 8). In that study, all scFvs were derived from a single clone, C6.5, with affinities for the same HER2 epitope ranging from 3.2×10^{-7} to 1.5×10^{-11} mol/L in approximately logarithmic steps (9, 10). Selective tumor targeting required at least 10^{-8} mol/L affinity, but further stepwise increases in affinity did not appreciably improve quantitative tumor retention. Moreover, we found that changes in affinity are sufficient to limit both the total uptake and the distance an scFv can penetrate into a tumor (8).

While divalent binding of scFv dimers greatly increases tumor retention (11), no comprehensive study has been conducted to date that describes the relationship between IgG affinity, uptake, and penetration *in vivo*. In work presented here, we examine the *in vivo* tumor uptake and penetration of anti-HER2 IgG molecules derived from the C6.5 scFv series of affinity mutants (12). All of the C6.5-derived IgGs share the same Fc domains and target the same epitope on HER2 and differ only in single point mutations in the complementarity determining regions (CDR). Here we extend these studies by examining the impact of affinity on the *in vivo* tumor-targeting properties of intact immunoglobulin molecules. We show that high affinity does not improve quantitative tumor targeting but does promote antibody internalization and degradation, limiting the tumor penetration of antibodies from blood vessels.

Material and Methods

Antibodies, cell lines, and radiolabeling

C6.5 IgG1 affinity variants were produced and characterized exactly as described previously (12). Trastuzumab (Herceptin) was obtained through the Fox Chase Cancer Center's pharmacy and diluted to 1 mg/mL prior to use. Before radiolabeling of the C6.5 variants, storage buffer was exchanged to sterile PBS, using 4-mL 10,000 MWCO Amicon centrifugal filters (Millipore). No buffer exchange was conducted on trastuzumab. For radioiodination reactions, 1 μ Ci 125 I-Na (Perkin-Elmer) per μ g of IgG to be labeled was dissolved in 50 μ L of 0.2 mol/L phosphate buffer (pH 7.6), applied to Pierce Pre-Coated Iodination Tubes (Thermo Scientific), and mixed at room temperature (RT) for 5 minutes. The IgG was added to the iodination tube and mixed for 3 minutes at RT. The labeling reaction was terminated by removal of protein from iodination tube followed by purification over a Sephadex G-50 spin column (Sigma) preequilibrated with PBS (pH 7.4). The SK-OV-3 cell line (ATCC HTB-77) was obtained from the American Type Culture Collection (ATCC) and was passaged for fewer than 6 months. The

ATCC has verified the identity of this cell line by methods including short tandem repeat profiling.

Prior to radiometal chelation, trace metal contaminants were removed from all buffers and water by passage over a 2.5×50 -cm column (Kontes) with Chelex 100 resin (Bio-Rad). All IgGs were exchanged into 500 mmol/L NaCl, 50 mmol/L carbonate buffer (pH 8.5), and conjugated with a 50-fold molar excess of CHX-A'-DTPA (Macrocyclics) for 18 hours at RT in the dark. Excess chelator was removed by buffer exchange, 4 times, into 150 mmol/L acetate buffer (pH 5.3). With specific activity diluted to 20 μ Ci/ μ L in 50 mmol/L HCl, 111 InCl₃ (Perkin-Elmer) was added to 500 mmol/L acetate buffer to yield 111 InOAc in 150 mmol/L buffer. At a ratio of 1.2 μ Ci/ μ g, IgG-DTPA conjugate was mixed with 111 InOAc for 18 hours at RT in the dark. Excess 111 In was chelated with the addition of 100 mmol/L EDTA (final concentration 5–10 mmol/L) and separated over Sephadex column as described earlier.

Quality control of the radiolabeled antibodies was done as previously described (8). Briefly, purity of all radiolabeled proteins was assessed using TEC-Control Chromatography Strips (Biodex). Immunoreactivity (IR) after labeling was verified by assaying 10 ng labeled IgG against 3×10^6 SK-OV-3 cells and determining percent bound to cells and supernatant. The average %IR after radioiodination reactions from multiple studies was 52.9%, 77.4%, 57.3%, 65.7%, and 87.9% for G98A, C6.5, ML39, H3B1, and trastuzumab, respectively. The average %IR after radioindium chelation from multiple studies was 56.1%, 71.2%, 62.3%, 70.3%, and 62.2% for G98A, C6.5, ML39, H3B1, and trastuzumab, respectively.

Internalization assays

SK-OV-3 cells were harvested in the logarithmic phase of growth and incubated with the 125 I-labeled IgGs at 450 ng per 5×10^5 cells on ice for 1 hour. Cells were washed twice with cold PBS containing 1% bovine serum albumin, aliquoted to 18 tubes, and incubated at 37°C, 5% CO₂. After 0, 1, 2, 4, 8, and 24 hours, the cultures were separated into catabolized, dissociated, cell surface-bound, and internalized fractions as described later. Cell suspensions were pelleted in a refrigerated centrifuge at 1,500 rpm for 5 minutes. Supernatants were transferred to Microcon YM-30 centrifugal filter unit (Millipore), followed by centrifugation at 14,000 rpm for 20 minutes. The supernatants, which passed through the filters, represented the catabolized fractions, whereas what remained in the filters comprised the dissociated fractions. Cell surface-bound IgGs were eluted from cell pellets with freshly made stripping buffer (2 mol/L urea, 50 mmol/L glycine, 150 mmol/L NaCl, pH 2.4). The elution step was repeated 3 times to remove over 98% of cell surface antibodies. The cell pellets after elution contained the internalized fractions. All the fractions were assayed in a Packard E5002 gamma counter (Perkin-Elmer).

Biodistribution studies

Antibody biodistribution studies were conducted as previously described (13). Four- to 6-week-old female SCID (severe combined immunodeficient) mice were obtained from the Fox Chase Cancer Center Animal Facility. Tumors

were implanted by subcutaneous (s.c.) injection of 2.5×10^6 SK-OV-3 cells into the abdomen of the mice. After 6 to 8 weeks, the tumors reached a size of 100 mg or larger. Mice to be used in ^{125}I experiments were given Lugol's solution in their drinking water to prevent thyroid accumulation of radioiodine. The pool of unoccupied Fc receptors in SCID mice was blocked by intraperitoneal (i.p.) administration of 1 mg murine IgG2a- κ (Sigma) to prevent altered pharmacokinetics. Biodistribution studies were initiated 48 hours later with the intravenous injection of 20 μg radiolabeled antibody. Within 5 to 10 minutes, blood samples were taken and whole-body counts were measured on a Captus 600 or Captus 3000 multichannel analyzer (Capintec) to determine the total injected dose. For analysis of the full C6.5 IgG affinity series, tumor, tissue, and blood distribution were assessed at 24 and 120 hours. For C6.5 and trastuzumab time course experiments, these measurements were taken at 8, 24, 48, 72, and 120 hours after injection. Cohorts of 5 mice were employed at each time point, and blood samples were taken immediately before euthanasia. Immediately after euthanasia, whole-body counts were measured and tumors and normal organs were removed and weighed. The percent injected dose per gram (%ID/g) was determined as previously described (14) for each organ and blood sample after determining the cpm (counts per minute) retained in the samples using a Packard E5002 gamma counter (Perkin-Elmer). All measurements were corrected for radioactive decay. Representative results from multiple studies are shown. Statistical significance was determined by an unpaired *t* test using GraphPad software.

Immunohistochemistry penetration studies

With the exception of Lugol's solution, mice and tumors were handled as described earlier. Antibodies were obtained and buffer exchanged to sterile PBS as described earlier. Consistent with previous models of tumor penetration (8), 500 μg of each antibody was injected i.p. into cohorts of 3 mice 48 hours after administration of the blocking IgG2a- κ . After 120 hours, mice were euthanized and tumors removed and fixed in 10% formalin for 24 to 48 hours. After embedding in paraffin blocks, sections were cut and mounted on slides for Immunohistochemistry (IHC). After deparaffination and rehydration using standard methodologies, primary antibodies were applied. Human HER2 (hHER2) was detected using rabbit anti-human c-erbB-2 oncoprotein polyclonal antibody (A0485; Dako). Blood vessels were detected using rat anti-mouse CD31 (553370; BD Pharmingen) mAb. The i.p. administered antibodies were detected in tumor sections with biotinylated goat anti-human IgG antibodies (Vector Labs). For double staining of CD31 and human IgG, the sections were treated with 0.06% Pronase E (Sigma) in 0.5 mol/L Tris buffer, pH 7.5, for 10 minutes at RT and then incubated with 3% H_2O_2 for 10 minutes to block endogenous peroxidase activity. Sections were blocked with normal rabbit serum. Tumor sections were incubated with rat anti-mouse CD31 (PECAM-1) mAb at a 1:300 dilution overnight at 4°C. Negative controls were incubated with the rat serum IgG at the same protein

concentration. All sections were washed in PBS containing 0.05% Tween-20 and then incubated with goat anti-rat IgG (BD Pharmingen) at a 1:200 dilution for 30 minutes at RT. After washing, the sections were incubated in an avidin peroxidase reagent (SA-HRP 1:100 dilution; Perkin Elmer) for 30 minutes. After washing, a Biotinyl-Tyramide enhancement kit (TSA Biotin Tyramide Reagent Pack; Perkin Elmer) was used according to the manufacturer's instructions. After washing, the sections were incubated in peroxidase substrate (3,3'-diaminobenzidine; Sigma) for 5 minutes. Next, we used biotinylated goat anti-human IgG, dilution 1:4,000, overnight at 4°C followed by streptavidin peroxidase reagent (Bio Genix) that was developed with the Vector VIP substrate for peroxidase as per manufacturer's instructions (Vector Labs). This produces a purple immunostaining that contrasted with the brown stain of CD31 blood vessels. The average tumor penetration of the mAbs was quantified using deidentified samples by measuring the distance of anti-human IgG staining from blood vessels. For each mAb, 4 isolated blood vessels were randomly selected per slide on 3 different slides (2 for ML39). The distance (in μm) the mAbs penetrated was measured twice for each vessel with each measurement taken on opposite sides, resulting in 8 measurements per slide. Statistical significance was determined using an unpaired *t* test using GraphPad software.

Results

High-affinity IgG exhibits less tumor retention and accumulation than moderate affinity clones *in vivo*

To probe the relationship between IgG binding affinity and tumor retention, a panel of anti-HER2 IgGs derived from a series of C6.5 scFv affinity variants (9, 10) was utilized (Supplementary Table S1). At the amino acid sequence level, the series of IgGs derived from the C6.5 clone are identical except for point mutations in the CDR affecting affinity to HER2. Similar to their parental scFv clones, these IgGs all target the same epitope on HER2 with distinct logarithmic increases in monovalent binding affinity from 270 to 0.56 nmol/L. With the exception of the lowest-affinity IgG, only minor differences in the functional (bivalent) affinities of the IgGs were observed (12). This was likely due to the limitations of the assays available to accurately measure very high multivalent affinities. For the reason of clarity, our observations will be discussed predominantly in consideration of IgG monovalent binding affinity; however, it should be noted that bivalent affinity is likely playing a significant role in our observations.

To determine tumor uptake, 20- μg radioiodinated (^{125}I) anti-HER2 IgGs were injected intravenously into SCID mice with established s.c. SK-OV-3 human ovarian carcinoma tumor xenografts overexpressing HER2. For each mAb [G98A (270 nmol/L), C6.5 (23 nmol/L), ML39 (7.3 nmol/L), and H3B1 (0.56 nmol/L)], cohorts of 5 mice were euthanized after 24 and 120 hours, and the amount of radiolabeled antibody remaining in tumors, normal tissue, and circulation was determined. Multiple studies were

Table 1. Biodistribution of ^{125}I -labeled anti-HER2 antibodies

	G98A		C6.5		ML39		H3B1	
	24 h	120 h	24 h	120 h	24 h	120 h	24 h	120 h
Blood	10.4	6.4	10.9	5.8	13.4	7.6	9.9	4.4
Tumor	6.8	5.6	7.7	6.5	6.7	5.9	5.5	3.1
Liver	3.3	2.1	4.0	2.3	4.1	2.5	3.6	1.7
Lung	9.9	5.7	10.0	4.8	11.3	5.9	8.7	3.3
Spleen	2.9	1.6	1.4 ^a	1.5	2.5	1.6	2.4	0.9
Kidney	3.0	1.9	3.1	1.9	3.2	2.1	2.6	1.1
Heart	5.2	3.7	5.5	2.9	5.5	3.3	4.5	2.0
Stomach	1.5	1.2	1.6	1.2	1.8	1.1	1.3	0.7
Bone	1.2	0.8	1.2	0.7	1.0	0.8	1.0	0.5
Intestine	1.5	1.2	1.5	1.0	1.5	1.1	1.4	0.6
Muscle	1.2	0.8	1.1	0.7	0.8	0.7	0.7	0.4

NOTE: The average %ID/g of radioiodinated antibody in each organ is listed 24 and 120 hours after injection. SEM is less than 20% of the average %ID/g except where noted (^a, SEM = 0.36).

Downloaded from <http://aacrjournals.org/cancerres/article-pdf/71/6/2250/2662737/2250.pdf> by Rockefeller University user on 07 March 2026

conducted, and the results of a representative experiment are shown in Table 1 and Figure 1. Although no consistent difference in accumulation in normal tissue or rates of systemic clearance was observed for the anti-HER2 affinity series (Table 1), it was repeatedly observed that the high-affinity IgG H3B1 (0.56 nmol/L monovalent K_D) had the significantly lower tumor accumulation at both 24 hours ($P = 0.0476$) and 120 hours ($P < 0.0001$; Fig. 1, dark gray bars) than C6.5 IgG (Fig. 1, light gray bars). The low- and moderate-affinity IgGs G98A and ML39 (270 and 7.3 nmol/L monovalent K_D , respectively) had slightly lower

accumulation in the tumor than C6.5, although these differences were not statistically significant (Fig. 1, black and white bars).

IgG binding affinity limits penetration into tumors *in vivo*

Although the biodistribution study described earlier revealed varying tumor retention of antibodies based on antibody intrinsic affinity, it cannot address antibody localization within the tumors. Therefore, to investigate the relationship between the distance an antibody penetrates into the tumor from a blood vessel and affinity, we administered a 500 μg i.p. dose of the each unlabeled affinity variant and trastuzumab to SCID mice bearing established SK-OV-3 tumors. After 120 hours, tumors were harvested and stained for hHER2, tumor vasculature (CD31), and human IgG to determine antibody penetration as a function of affinity (Fig. 2). IHC revealed no significant differences in tumor structure (Fig. 2A) or in the relative expression of hHER2 on the surface of the tumor cells (Fig. 2B). Dual staining (Fig. 2C-H) for the blood vessels (CD31, brown) and for human IgG (purple) revealed significant differences in the penetration of the antibodies from blood vessels into the tumor with an apparent threshold occurring between 23 and 7.3 nmol/L monovalent affinity. G98A, the mAb with the lowest monovalent affinity (270 nmol/L), exhibited the greatest average penetration distance from the blood vessels (84.8 μm). C6.5, the mAb with a moderate monovalent affinity (23 nmol/L), penetrated to an average distance of 59.7 μm . Further increases in monovalent affinity (e.g., ML39, 7.3 nmol/L; H3B1, 0.56 nmol/L; and trastuzumab, 0.09 nmol/L) were associated with significantly decreased tumor penetration (23.3, 20.4, and 37.2 μm , respectively; $P < 0.0001$ for C6.5 IgG vs. all other antibodies). This observed degree of tumor penetration is within the predicted range modeled by others (based upon published data sets from a number of groups) of approximately 20 and 130 μm when a

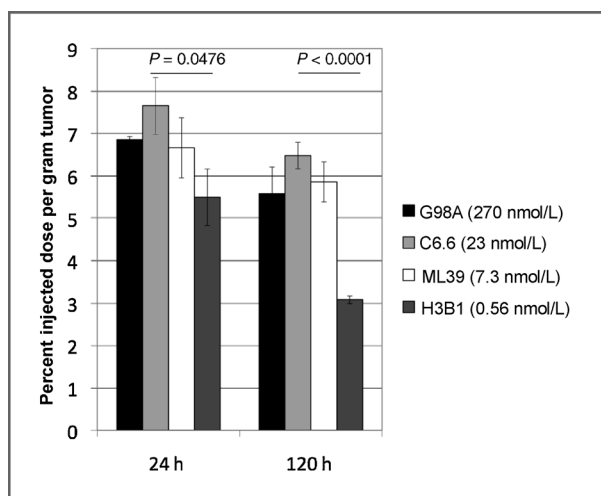


Figure 1. Affinity limits the tumor uptake of antibodies. For each anti-HER2 affinity variant, 20 μg ^{125}I -labeled IgG was injected into SCID mice bearing s.c. SK-OV-3 tumors. The amount of antibody in tumors was determined at 24 hours (left) and 120 hours later (right). The monovalent affinity, as previously determined by SPR, is given for each antibody in the graph key. The statistical significance (P) in comparing C6.5 to H3B1 is given above each time point. The average of 5 mice \pm SEM is graphed per point.

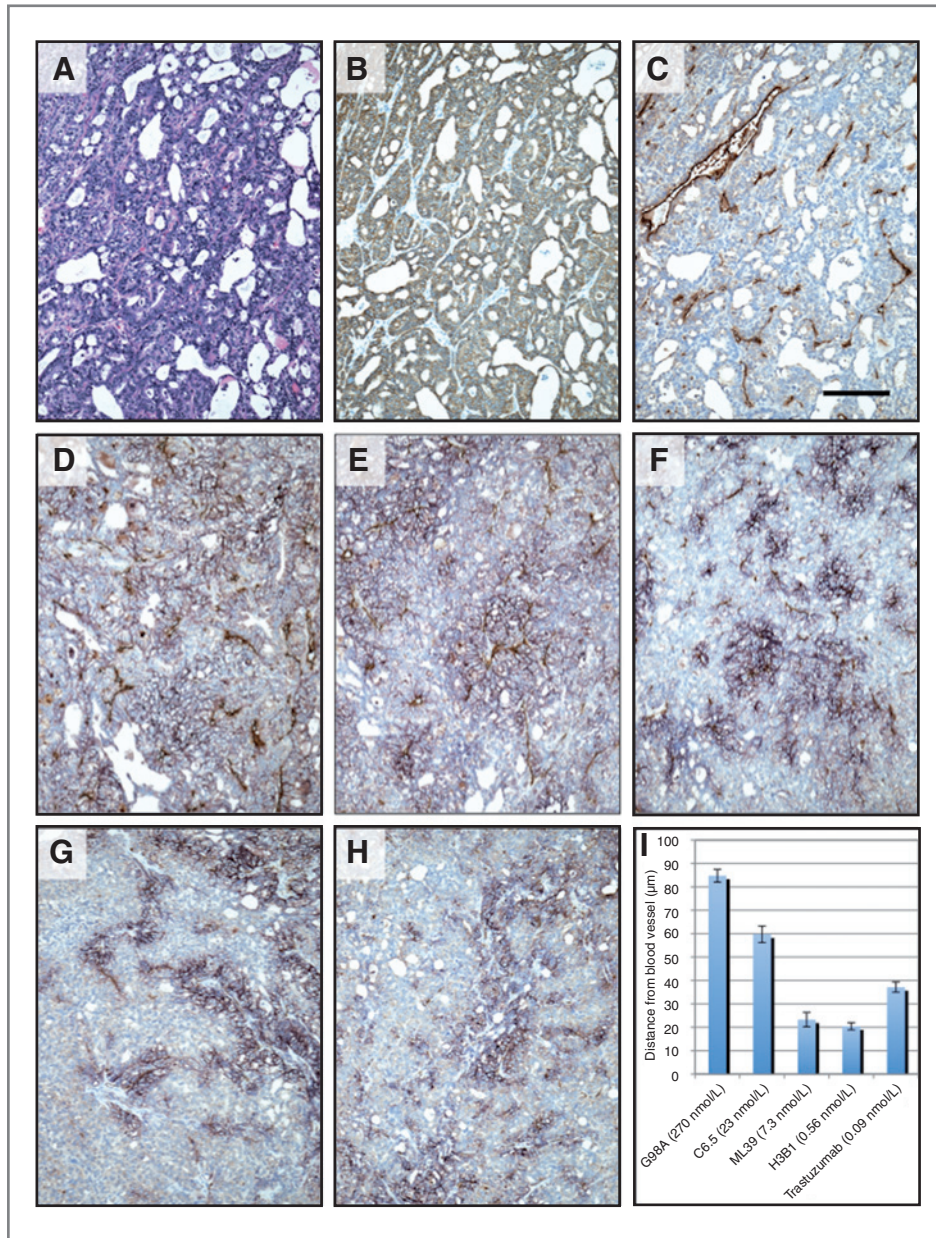


Figure 2. Affinity limits antibody penetration into tumors. Representative IHC of s.c. SK-OV-3 tumors 120 hours after i.p. injection of 500 µg of anti-HER2 IgG. Adjacent sections of tumors from untreated mice were stained with hematoxylin and eosin (A) and for hHER2 (B). Dual staining for blood vessels (brown) and human IgG (purple) was carried out on tumors from untreated mice (C) and mice treated with G98A (D), C6.5 (E), ML39 (F), H3B1 (G), and trastuzumab (H). The bar in panel C represents 100 µm with 10× magnification. I, the plots of average distance (±SEM) of IgG penetration from randomly selected blood vessels.

500-µg dose is governed by antigen turnover and systemic clearance, respectively (5).

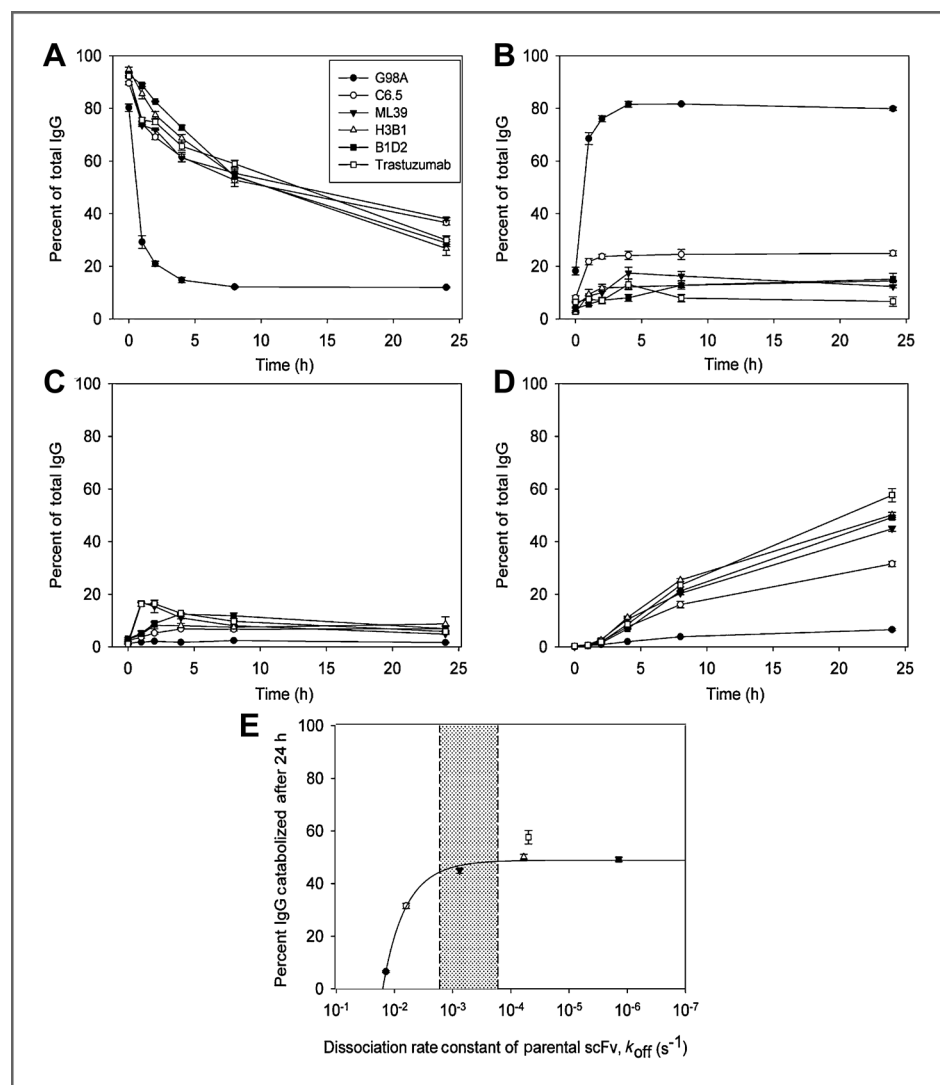
Affinity and the rate of antigen internalization dictate the subcellular distribution of anti-HER2 IgGs

Antigen-mediated internalization of antibodies has been shown to lead to their degradation in a variety of models *in vitro* (4, 15, 16) and *in vivo* (17). Furthermore, HER2 is a dynamic antigen whose internalization varies with receptor states, such as hetero/homodimerization, and ligand binding (18) but is not affected by binding of trastuzumab (19). Therefore, to investigate the impact of antibody affinity on subcellular distribution, an internalization assay was conducted with ¹²⁵I-labeled IgGs as previously described (19).

For the C6.5 variants and trastuzumab, 450 ng ¹²⁵I-labeled IgG was incubated with 5×10^5 SK-OV-3 cells and the degree of catabolism, dissociation, retention on the cell surface, and retention inside of cells were determined after 0, 1, 2, 4, 8, and 24 hours.

With the exception of the lowest affinity antibody G98A, 60% to 70% of each IgG remained on the cell surface within the first 4 hours of the assay (Fig. 3A). After 24 hours, however, more C6.5 and ML39 remained on the surface of the cells than was observed with the highest affinity variants (H3B1 and BID2) and trastuzumab. More than 80% of G98A dissociated in 4 hours (Fig. 3B), explaining why so little was observed on the cell surface. In contrast, C6.5 dissociated slower than G98A and the highest affinity variants and trastuzumab (Fig. 3B)

Figure 3. Affinity, relative to the rate of antigen internalization, determines the extent of antibody catabolism *in vitro*. Internalization assays were conducted by incubating 450 ng ^{125}I -labeled anti-HER2 IgGs with 5×10^5 SK-OV-3 cells. Samples were taken immediately following or 1, 2, 4, 8, and 24 hours after unbound IgG was washed from cells. The percentage of total antibody is shown with respect to time for surface bound (A), dissociated (B), internalized (C), and degraded (D) antibody. The average ± 1 SD is shown from triplicate samples. The correlation of degradation with antigen internalization (E) was made by plotting the 24 hours time point (as in D) against the SPR determined rate of dissociation of the parental scFv from each affinity clone. The monovalent scFv affinity used for trastuzumab (unfilled square) was determined for the 4D5 Fab elsewhere (28). The region shaded in gray represents the range of internalization rates (k_e) as determined by others (18).



exhibited the least dissociation. Very little of any of the IgGs remained intact inside the cells despite their large differences in affinity (Fig. 3C). Because of pronounced dissociation from the cells, very little G98A was degraded (Fig. D). The degradation of the other tested IgGs increased over time. Since the monovalent dissociation rate constant (k_{off}) for the IgGs has not been measured, catabolism after 24 hours was correlated with the k_{off} rate of the parental scFv molecules. For G98A, C6.5, and ML39 with scFv-based off rates faster than $7 \times 10^{-4} s^{-1}$ (10), catabolism increased with affinity (decreased off rate; Fig. 3E). For mAbs with slower rates of dissociation, H3B1, B1D2, and trastuzumab (20), catabolism and degradation were no longer impacted by further decreases to the off rate.

Reported HER2 internalization rates (k_e) range from 1.6×10^{-3} to $1.6 \times 10^{-4} s^{-1}$ (18) and are represented in Figure 3 by the shaded region. This suggests that the rate of HER2 internalization serves as an affinity threshold in determining the fate of these antibodies. Degradation increases with affinity as long as the k_{off} is faster than k_e despite the ability of the antibodies to bind bivalently. Furthermore, internaliza-

tion is independent of affinity and becomes totally antigen dependent when k_{off} is slower than k_e , and these interactions, as with many other antibodies, can be considered irreversible as suggested previously by others (15, 16).

Pharmacokinetic analysis reveals that tumors consume significant amounts of antibody *in vivo*

Of the antibodies that showed significant retention on the surface of SK-OV-3 cells, C6.5 IgG exhibited the least degradation whereas trastuzumab exhibited the highest level. We hypothesized that this would lead to distinct rates of uptake and clearance stemming from the more rapid turnover of trastuzumab relative to C6.5. To address this hypothesis, 2 biodistribution experiments were conducted to compare the systemic and tumor pharmacokinetics of C6.5 and trastuzumab. These experiments were designed to exploit the metabolic differences between ^{125}I and ^{111}In radiolabels in order to determine the relative impacts of internalization and degradation. Once internalized, radio-iodotyrosine metabolites from ^{125}I -labeled mAbs are rapidly eliminated by cells

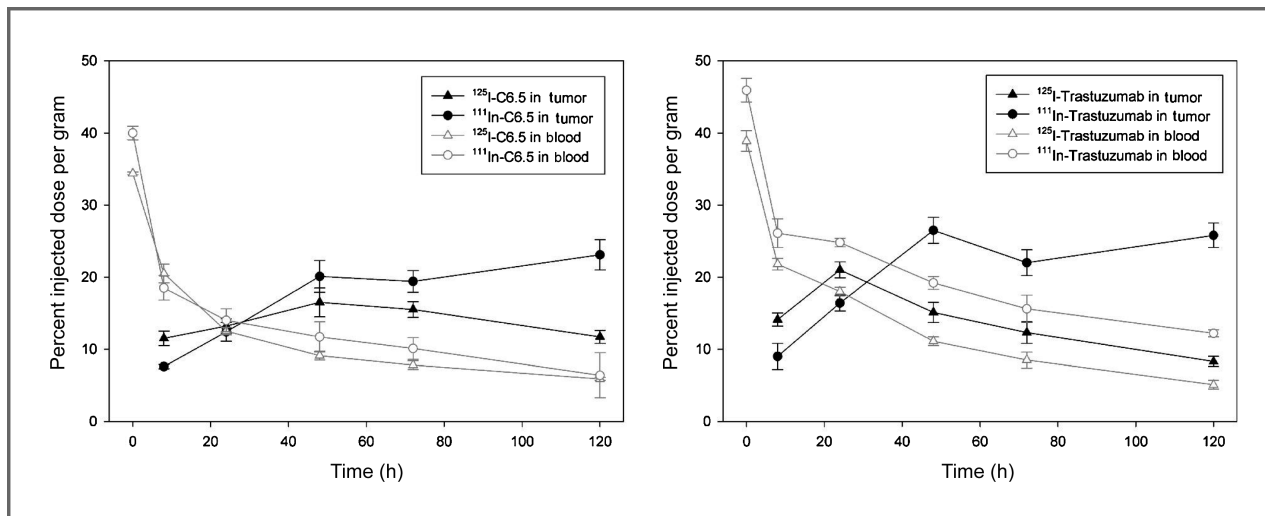


Figure 4. Comparison of radiolabel reveals that tumors consume significant amounts of antibody *in vivo*. Biodistribution experiments were conducted as described in Figure 1. The $20\ \mu\text{g}$ of ^{125}I (triangles) or ^{111}In (circles)-labeled C6.5 IgG (left) and trastuzumab (right) were injected into SCID mice bearing s.c. SK-OV-3 tumor xenografts. The amount of antibody in tumors (filled symbols and black line) and in circulation (empty symbols and gray line) was determined after 8, 24, 48, 72, and 120 hours. Each point is the average of 5 mice \pm SEM.

whereas radio-indium metabolites from ^{111}In -labeled mAbs residualize and accumulate in cells following their degradation (21–23). Therefore, the ^{125}I radiolabel is representative of intact surface bound and unbound antibodies in the tumor microenvironment and the ^{111}In radiolabel is indicative of both intact and the accumulated degraded antibodies.

In Figure 4, the %ID/g in blood (empty symbols with gray lines) and in tumor (filled symbols with black lines) is presented for ^{125}I (triangles)- and ^{111}In (circles)-labeled C6.5 IgG (A) and trastuzumab (B). For both C6.5 and trastuzumab, the rate of clearance from circulation was independent of the radiolabel employed. Tumor accumulation of the radioiodinated antibodies peaked at 48 and 24 hours for C6.5 and trastuzumab, respectively. After 24 hours, ^{125}I -trastuzumab levels in the tumor decreased at the same rate as the antibody from circulation. In contrast, ^{125}I -C6.5 %ID/g in the tumor persisted at the same level between 48 and 72 hours despite much lower blood concentrations. Therefore, relative to trastuzumab, ^{125}I -C6.5 clearance from the tumor was delayed, even following first-pass clearance of both proteins. In contrast with the ^{125}I tumor retention profiles, between 48 and 120 hours, both antibodies possessed much higher ^{111}In tumor retention. Thus, both antibodies undergo *in vivo* internalization and degradation. Because of the increased rate of ^{125}I -trastuzumab clearance relative to C6.5, and the large difference between ^{125}I -trastuzumab (intact) and ^{111}In -trastuzumab (intact and degraded) accumulation in the tumor over time, we conclude that consistent with the *in vitro* data (Fig. 3), trastuzumab is internalized and degraded *in vivo* by tumors more than C6.5.

Total amount of antibody delivered to tumor *in vivo* is independent of affinity

On the basis of observations of the *in vitro* internalization assays and the pharmacokinetic study described earlier, the

higher-affinity clones should be degraded to a higher extent than lower-affinity clones *in vivo*. To test this hypothesis, an ^{111}In biodistribution study was conducted for the anti-HER2 affinity series (Fig. 5) to compare with the ^{125}I results presented in Figure 1.

For all IgGs, samples were collected 24 and 120 hours postinjection of $20\ \mu\text{g}$ ^{111}In -labeled protein. Although no differences were observed in systemic clearance or normal tissue distribution for the affinity variants (Table 2), the %ID/g of all the tested antibodies in the tumor increased over time.

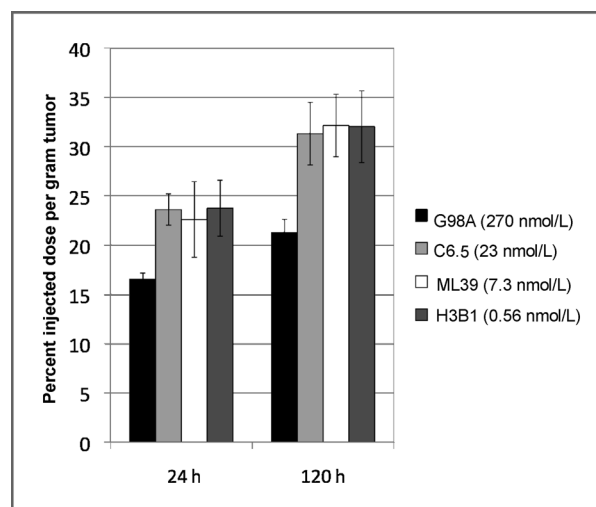


Figure 5. Use of residualizing isotope reveals that affinity does not limit the amount of antibody delivered to the tumor. For each anti-HER2 affinity variant, $20\ \mu\text{g}$ ^{111}In -labeled IgG was injected into SCID mice bearing s.c. SK-OV-3 tumors. The amount of antibody in tumors was determined 24 hours (left) and 120 hours later (right). The average of 5 mice \pm SEM is graphed per point.

Table 2. Biodistribution of ^{111}In -labeled anti-HER2 antibodies

	G98A		C6.5		ML39		H3B1	
	24 h	120 h	24 h	120 h	24 h	120 h	24 h	120 h
Blood	16.8	9.1	15.8	8.3	22.2	15.5	18.1	9.0
Tumor	16.6	21.3	23.6	31.3	22.6	32.1	23.7	32.0
Liver	6.3	4.9	5.8	3.4	8.3	6.7	6.8	6.2
Lung	11.1	7.4	14.6	8.4	17.6	12.9	15.9	6.3
Spleen	6.9	7.2	7.0	5.7	8.2	8.2	6.3	6.0
Kidney	5.7	5.2	5.4	3.9	6.8	4.8	6.1	4.0
Heart	7.9	5.7	8.0	4.9	7.8	4.3	7.5	3.6
Stomach	2.6	1.8	2.7	1.6	2.8	2.0	2.4	1.7
Bone	2.0	1.8	2.1	1.6	3.1	1.8	2.6	1.9
Intestine	2.1	2.0	2.7	1.7	2.8	2.6	2.8	2.1
Muscle	1.8	1.5	1.6	1.2	1.5	0.9	1.3	1.2

NOTE: The average %ID/g of radio-indium-labeled antibody in each organ is listed 24 and 120 hours after injection. In all cases, SEM is less than 20% of the average %ID/g.

Downloaded from <http://aacrjournals.org/cancerres/article-pdf/71/6/2250/2662737/2250.pdf> by Rockefeller University user on 07 March 2026

Accordingly, factors such as extravasation from blood vessels were apparently unaffected by affinity. For the 3 IgGs with monovalent K_D below 10^{-8} mol/L, the accumulation of the ^{111}In -labeled forms in tumor, comprising both intact and degraded IgGs, was identical whereas ^{111}In -G98A tumor accumulation was significantly lower ($P < 0.05$ for all 3 IgGs at 120 hours). In contrast with these results, affinity higher than that of C6.5 IgG leads to the tumor retention of less intact radioiodinated antibody because of *in vivo* internalization and degradation, illustrating the magnitude of escalating mAb degradation by the tumors as affinity increases from C6.5 to H3B1.

Discussion

To the best of our knowledge, this is the first thorough examination of the effects of affinity on *in vivo* tumor targeting of intact IgG molecules. In the studies described earlier, we have determined that the intrinsic affinity of intact IgG molecules is a critical determinant in the accumulation and penetration into solid tumors *in vivo*. Working with a series of IgG molecules spanning a wide range of intrinsic affinity for the same target epitope, we found that as the affinity of the antibody for its target antigen increased, the distribution became more perivascular in nature. Furthermore, as the higher-affinity antibodies exhibited a greater degree of internalization and catabolism in both our *in vitro* and *in vivo* studies, we postulate that the limited penetration of the higher-affinity antibodies was due to their more efficient catabolism and degradation by the perivascular tumor cells. Antibodies that exhibit efficient penetration into solid tumors would likely target a greater proportion of the tumor, potentially exhibiting improved therapeutic efficacy. Accordingly, the data presented here provide a context for understanding how to design antibodies for specific applications that require either perivascular targeting or thorough tumor penetration.

The role of affinity in tumor targeting with antibody-based molecules has been the subject of significant study and interest. However, until now, these studies have been conducted with antibodies that target different epitope on the tumor antigen (24) or with antibody fragments or targeting molecules based on alternate scaffolds (8, 25, 26). These studies offered important insights into the impact of affinity. For example, we observed that scFv with high affinities exhibit distinct perivascular accumulation whereas low-affinity scFvs show a broad, almost homogenous, distribution throughout the vascularized regions of the tumor (8). However, this prior work did not provide direct evidence for the role of affinity in tumor targeting by intact IgG molecules. Targeting different epitopes with different affinity IgGs could bias the outcome of the studies by altering biological processes such as the rates of internalization and recycling. The use of fragments such as scFv molecules or alternative scaffolds such as Affibodies or DARPins would be subject to different rates of systemic elimination due to differences in size, lack of interaction with the immunoglobulin salvage receptor FcRn, and varied sites of catabolism. The studies described in this article were specifically designed to definitively test the impact of intrinsic affinity for a targeted tumor antigen on the ability of IgG molecules to target tumors in the *in vivo* setting. By using a panel of antibodies that exhibited specificity for identical epitopes of HER2 ECD, and were nearly identical in their sequences and structure, we were able to isolate and assess the influence of affinity.

In the current study, analyzing the behavior of bivalent IgGs offered both familiar and new insights into how antibodies target and distribute throughout tumors. First, we observed that, using the same *in vivo* model as was used for scFv studies described earlier, increasing affinity again did not enhance tumor uptake. In fact, ^{125}I -labeled H3B1, the highest affinity IgG that was tested, had less tumor accumulation than the other affinity variants and this difference grew between 24 and

120 hours (Fig. 1). Next, as with the scFv in previous studies, it was observed that high-affinity IgGs have less penetration than do their lower-affinity counterparts. Interestingly, there seems to be a threshold between the C6.5 (intrinsic affinity = 23 nmol/L) and ML39 (intrinsic affinity = 7.3 nmol/L) IgGs in our model that distinguishes more tumor-penetrative mAbs from the more perivascularly retained mAbs (Fig. 2). This observation clearly implies the existence of a binding site barrier in this system but does not explain the mechanistic basis for the observation.

To address this issue, *in vitro* internalization assays were conducted (Fig. 3). These studies have shown that G98A, and to a lesser extent C6.5, dissociate from the surface of the cells more completely than their higher-affinity counterparts. This likely explains why these antibodies distributed more widely throughout the tumors as assessed by IHC. In contrast, ML39, H3B1, and trastuzumab were extensively degraded *in vitro* by tumor cells and exhibited limited *in vivo* tumor penetration. Furthermore, these higher-affinity antibodies possessed rates of monovalent dissociation that were slower than the reported internalization rate of HER2 (Fig. 3E). Although the binding of antibodies to shed antigen within the tumor interstitial space has been shown to block the function of the antibodies in some tumors (27), the differences we observed in the tumor uptake of the antibodies labeled with residualizing and non-residualizing radioisotopes suggest that this was not a defining limitation in the current study. These findings suggest that irreversible binding of antigen due to internalization and degradation by tumor cells contributes to the "binding site barrier" that limits penetration into the tumor.

Antibody internalization and degradation led to the impressive *in vivo* consumption of mAb by tumors (Fig. 4). We found that trastuzumab was more efficiently degraded than C6.5, even though the 2 antibodies have similar measured functional affinities (12). Although the antibodies bind to distinct HER2 epitopes, they also differ in intrinsic binding site affinity by 255-fold, either property may be responsible for more complete internalization and degradation of trastuzumab. These observations, coupled with the limited perivascular tumor penetration of trastuzumab, are consistent with models illustrated by others (see Fig. 2 in ref. 16). However, there is a lag in the tumor clearance

of C6.5 after mAb levels decrease in circulation (Fig. 4). We speculate that this could be due to the rapid rate of C6.5 dissociation relative to the rate of HER2 internalization by the targeted tumor cells. As shown in Figure 1, it is evident that as affinity increases, so does *in vivo* consumption of the antibody by the tumor. Future studies should consider the total exposure of an mAb to cancer cells as a true area under the (concentration vs. time) curve for the tumor itself and not rely on a single time point.

Although the ultimate correlation of affinity and penetration with efficacy requires additional studies, we have shown a clear structure: function relationship between an mAb and its target wherein the antibody's intrinsic binding affinity has a tangible impact on distribution and therefore *in vivo* exposure of tumor to drug. The ultimate applicability of these observations depends on numerous factors including the relationship of targeting to efficacy, the internalization rate of the targeted antigen, and the targeted antigen's expression density. Despite these caveats, the studies presented here describe principles that should be considered when designing mAb for imaging or therapeutic applications.

Disclosure of Potential Conflicts of Interest

No potential conflicts of interest were disclosed.

Acknowledgments

We thank Catherine Renner and Huaifen Li of the Fox Chase Cancer Center (FCCC) Histopathology Core Facility, the members of the FCCC Laboratory Animal Facility and Kim Boland, Heidi Simmons, and R. Brian Freer of the FCCC Developmental Therapeutics Program for their excellent technical assistance. We also thank Dr. Matthew Robinson of FCCC for helpful discussions.

Grant Support

This work was supported by NCI grants R01 CA118159 (G.P. Adams), R01 CA50633 (L.M. Weiner), NIH T32 CA009035 (S.I. Rudnick), the Bernard A. & Rebecca S. Bernard Foundation and an appropriation from the Commonwealth of Pennsylvania.

The costs of publication of this article were defrayed in part by the payment of page charges. This article must therefore be hereby marked *advertisement* in accordance with 18 U.S.C. Section 1734 solely to indicate this fact.

Received June 28, 2010; revised December 1, 2010; accepted January 2, 2011; published online March 15, 2011.

References

- Fujimori K, Covell DG, Fletcher JE, Weinstein JN. Modeling analysis of the global and microscopic distribution of immunoglobulin G, F(ab')₂, and Fab in tumors. *Cancer Res* 1989;49:5656-63.
- Fujimori K, Covell DG, Fletcher JE, Weinstein JN. A modeling analysis of monoclonal antibody percolation through tumors: a binding-site barrier. *J Nucl Med* 1990;31:1191-8.
- Jain RK. Physiological barriers to delivery of monoclonal antibodies and other macromolecules in tumors. *Cancer Res* 1990;50:814s-9s.
- Ackerman ME, Pawlowski D, Wittrup KD. Effect of antigen turnover rate and expression level on antibody penetration into tumor spheroids. *Mol Cancer Ther* 2008;7:2233-40.
- Thurber GM, Zajic SC, Wittrup KD. Theoretic criteria for antibody penetration into solid tumors and micrometastases. *J Nucl Med* 2007;48:995-9.
- Baker JH, Lindquist KE, Huxham LA, Kyle AH, Sy JT, Minchinton AI. Direct visualization of heterogeneous extravascular distribution of trastuzumab in human epidermal growth factor receptor type 2 over-expressing xenografts. *Clin Cancer Res* 2008;14:2171-9.
- Rudnick SI, Adams GP. Affinity and avidity in antibody-based tumor targeting. *Cancer Biother Radiopharm* 2009;24:155-61.
- Adams GP, Schier R, McCall AM, Simmons HH, Horak EM, Alpaugh RK, et al. High affinity restricts the localization and tumor penetration of single-chain Fv antibody molecules. *Cancer Res* 2001;61:4750-5.
- Schier R, Bye J, Apell G, McCall A, Adams GP, Malmqvist M, et al. Isolation of high-affinity monomeric human anti-c-erbB-2 single chain Fv using affinity-driven selection. *J Mol Biol* 1996;255:28-43.
- Schier R, McCall A, Adams GP, Marshall KW, Merritt H, Yim M, et al. Isolation of picomolar affinity anti-c-erbB-2 single-chain Fv by mole-

- cular evolution of the complementarity determining regions in the center of the antibody binding site. *J Mol Biol* 1996;263:551–67.
11. Adams GP, Tai MS, McCartney JE, Marks JD, Stafford WF III, Houston LL, et al. Avidity-mediated enhancement of *in vivo* tumor targeting by single-chain Fv dimers. *Clin Cancer Res* 2006;12:1599–605.
 12. Tang Y, Lou J, Alpaugh RK, Robinson MK, Marks JD, Weiner LM. Regulation of antibody-dependent cellular cytotoxicity by IgG intrinsic and apparent affinity for target antigen. *J Immunol* 2007;179:2815–23.
 13. Adams GP, Schier R, Marshall K, Wolf EJ, McCall AM, Marks JD, et al. Increased affinity leads to improved selective tumor delivery of single-chain Fv antibodies. *Cancer Res* 1998;58:485–90.
 14. Adams GP, Denardo SJ, Amin A, Kroger LA, DeNardo GL, Helström I, Helström KE. Comparison of the pharmacokinetics in mice and the biological-activity of murine L6 and human-mouse chimeric Ch-L6 antibody. *Antib Immunoonjug Radiopharm* 1992;5:81–95.
 15. Kyriakos RJ, Shih LB, Ong GL, Patel K, Goldenberg DM, Mattes MJ. The fate of antibodies bound to the surface of tumor cells *in vitro*. *Cancer Res* 1992;52:835–42.
 16. Thurber GM, Schmidt MM, Wittrup KD. Antibody tumor penetration: transport opposed by systemic and antigen-mediated clearance. *Adv Drug Deliv Rev* 2008;60:1421–34.
 17. Lammerts van Bueren JJ, Bleeker WK, Bogh HO, Houtkamp M, Schuurman J, van de Winkel JG, et al. Effect of target dynamics on pharmacokinetics of a novel therapeutic antibody against the epidermal growth factor receptor: implications for the mechanisms of action. *Cancer Res* 2006;66:7630–8.
 18. Hendriks BS, Opresko LK, Wiley HS, Lauffenburger D. Quantitative analysis of HER2-mediated effects on HER2 and epidermal growth factor receptor endocytosis: distribution of homo- and heterodimers depends on relative HER2 levels. *J Biol Chem* 2003;278:23343–51.
 19. Austin CD, De Maziere AM, Pisacane PI, van Dijk SM, Eigenbrot C, Sliwkowski MX, et al. Endocytosis and sorting of ErbB2 and the site of action of cancer therapeutics trastuzumab and geldanamycin. *Mol Biol Cell* 2004;15:5268–82.
 20. Kubetzko S, Balic E, Waibel R, Zangemeister-Wittke U, Pluckthun A. PEGylation and multimerization of the anti-p185HER-2 single chain Fv fragment 4D5: effects on tumor targeting. *J Biol Chem* 2006;281:35186–201.
 21. Mattes MJ, Griffiths GL, Diril H, Goldenberg DM, Ong GL, Shih LB. Processing of antibody-radioisotope conjugates after binding to the surface of tumor-cells. *Cancer* 1994;73:787–93.
 22. Press OW, Shan D, HowellClark J, Eary J, Appelbaum FR, Matthews D, et al. Comparative metabolism and retention of iodine-125, yttrium-90, and indium-111 radioimmunoconjugates by cancer cells. *Cancer Res* 1996;56:2123–9.
 23. Shih LB, Thorpe SR, Griffiths GL, Diril H, Ong GL, Hansen HJ, et al. The processing and fate of antibodies and their radiolabels bound to the surface of tumor-cells *in-vitro*—a comparison of 9 radiolabels. *J Nucl Med* 1994;35:899–908.
 24. Langmuir VK, Mendonca HL, Woo DV. Comparisons between two monoclonal antibodies that bind to the same antigen but have differing affinities: uptake kinetics and 125I-antibody therapy efficacy in multicell spheroids. *Cancer Res* 1992;52:4728–34.
 25. Zahnd C, Kawe M, Stumpp MT, de Pasquale C, Tamaskovic R, Nagy-Davidescu G, et al. Efficient tumor targeting with high-affinity designed ankyrin repeat proteins: effects of affinity and molecular size. *Cancer Res* 2010;70:1595–605.
 26. Friedman M, Stahl S. Engineered affinity proteins for tumour-targeting applications. *Biotechnol Appl Biochem* 2009;53:1–29.
 27. Zhang Y, Pastan I. High shed antigen levels within tumors: an additional barrier to immunoconjugate therapy. *Clin Cancer Res* 2008;14:7981–6.
 28. Kelley RF, O'Connell MP, Carter P, Presta L, Eigenbrot C, Covarrubias M, et al. Antigen binding thermodynamics and antiproliferative effects of chimeric and humanized anti-p185HER2 antibody Fab fragments. *Biochemistry* 1992;31:5434–41.